INFLUENCES OF STORM EROSION AND DEPOSITION ON RHYTHMITES OF THE UPPER WENCHANG FORMATION (UPPER ORDOVICIAN) AROUND TONGLU, ZHEJIANG PROVINCE, CHINA

DAIDU FAN,[1] CONGXIAN LI,[1] AND PING WANG[2]
[1] *Laboratory of Marine Geology, School of Ocean and Earth Science, Tongji University, Shanghai 200092, China*
e-mail: fandd@online.sh.cn
[2] *Department of Geology, University of South Florida, Tampa, Florida 33620, U.S.A.*

ABSTRACT: **Tonglu rhythmites (Upper Ordovician) in Zhejiang Province, east-central China, display three orders of cyclicity in sandstone and mudstone layer thickness. Millimeter-thick alternations of sandstone and mudstone laminae are ascribed to single tidal cycles. Centimeter-thick alternations of sand-dominated layers (SDLs) and mud-dominated layers (MDLs) are interpreted to be related to alternation of storm and calm weather conditions with a periodicity longer than that forced by neap–spring tidal cyclicity. The SDLs are interpreted as storm deposits on the basis of presence of scour structures, abundant intraformational mud pebbles, oscillation ripples, and thinning-upward trends in the sandstone laminae. A third, meter-thick cycle of variations in sandstone-lamina thickness is interpreted as a reflection of cross-shore changes in coastal dynamics and water depth in the subtidal–intertidal environment.**

Storm waves, usually considered to be random destructive factors to normal cyclic deposits, are here highlighted as effective agents of sediment transport and deposition of the sand-dominated layers. This study aims at improving our facies-level understanding of the genesis and preservation of storm-related tidal-flat rhythmites on open coasts, and highlights the fact that storm related facies can mimic the cyclicity that is commonly ascribed to neap–spring tidal variation.

INTRODUCTION

The term rhythmite was originally applied to rhythmic repetition of laminae or beds with different composition, texture, and color (Reineck and Singh 1980; Archer and Johnson 1997). Rhythmites have been described in a wide range of depositional facies, such as lacustrine varvites, shallow-marine storm deposits, and deep-water turbidites (Reineck and Singh 1980; Bhattacharyya et al. 1980). Rhythmites are also common in tide-influenced environments such as tidal flats and river estuaries. Termed ''tidal rhythmites'' to discriminate from others, such deposits display characteristic sedimentary structures such as bidirectional foresets in cross-beds, tidal bedding (including flaser, wavy, and lenticular forms), mud cracks, and raindrop imprints. Visser (1980) related the lateral rhythmic evolution of successive tidal-bundle thickness with neap–spring cycles. Since then, numerous rhythmites, ranging in age from Holocene to Proterozoic, have been examined quantitatively in terms of the patterns of variation in thickness of sand and mud laminae (e.g., Allen 1981; Allen and Homewood 1984; Yang and Nio 1985; Sonett et al. 1988; Kvale et al. 1989; Brown et al. 1990; Kuecher et al. 1990; Martino and Sanderson 1993; Archer 1994; Greb and Archer 1995; Miller and Eriksson 1997; Williams 1998; Kvale et al. 1999; Eriksson and Simpson 2000). In conjunction with laminae counts, harmonic analyses were used in most of the above studies to link the range of periodicities of lamina-thickness variations to semimonthly neap–spring cycles (Allen 1981; Kvale et al. 1989; Kvale and Archer 1990; Lanier et al. 1993; Martino and Sanderson 1993; Greb and Archer 1995; Miller and Eriksson 1997). In recent studies, the term ''tidal rhythmite'' was used specifically to refer to deposits that exhibit neap–spring cyclicity in the variation of lamina thickness. This quantitative characteristic, in turn, served as a criterion to indicate a tidal origin (e.g., Kvale et al. 1989; Brown et al. 1990; Kuecher et al. 1990; Miller and Eriksson 1997; Eriksson and Simpson 2000).

Allen and Duffy (1998), however, argued that the quantitative aspect of tidal rhythmites has been overemphasized to an extent that general lithological characteristics are sometimes overlooked. The neap–spring interpretation of the periodic variation in lamina thickness was also questioned by Bhattacharyya et al. (1980), Li et al. (2000), and Fan and Li (2002). These studies suggested that alternations of sand- and mud-dominated layers were caused by storm to calm-weather variations instead of neap–spring cycles. Storm waves are usually considered to be destructive agents, and few studies have linked them to cyclic deposits. Until now, storm deposits have been associated predominantly with shelf environments rather than tidal flats and salt marshes (Reineck and Gerdes 1997). Although storm deposits are commonly observed on tidal flats shortly after storm events, they tend to be reworked by tides, fair-weather waves, and bioturbation, which lower their preservation potential (Duke 1985). Nevertheless, storm deposits were found to be preserved in sheltered parts of tidal flats (Reineck and Gerdes 1997) and under conditions of rapid deposition (van den Berg 1981; Li et al. 2000; Fan et al. 2002).

In this study, sedimentary structures and characteristics of the sand–mud alternations in the Ordovician Tonglu rhythmites of SE China were examined in detail. Harmonic analyses of thickness variations in the sand laminae were conducted to identify possible tide-related periodicities and to examine the influences of storms in the deposition of the Tonglu rhythmites. In this paper, we demonstrate that the interpretation of tidal-flat rhythmites based solely on statistical analysis may be misleading. Detailed lithological characteristics and careful examination of regional paleoenvironment and sedimentary facies are crucial for the interpretation of periodicities of lamina-thickness variations identified by harmonic analysis. Our goal is to improve our facies-level understanding of the genesis and preservation of storm-related tidal-flat rhythmites along open coasts, which are more characteristic of global tidal sedimentation in the past, especially during Precambrian and early Paleozoic times (Klein 1975; Wells et al. 1990).

METHODS

Field descriptions of the Tonglu rhythmites include lithology, color, texture, and sedimentary structure. Thicknesses of individual laminae were measured over a section 6.7 m thick. Microscopic features including grain size, grain composition, grain fabric, and contact between adjacent laminae were examined in thin section and detailed sedimentary features were examined in polished hand specimens.

Time-series analysis based on the Fourier transformation was applied to examine the variation patterns of lamina thickness (cf. Yang and Nio 1985; Kvale and Archer 1990; Shi 1991; Archer 1994; Miller and Eriksson 1997; Kvale et al. 1999). The interpretation of the results of time-series analysis assumes that relatively high-energy spring tides would result in relatively thicker sand laminae whereas low-energy neap tides should result in thinner sand laminae.

STRATIGRAPHIC AND PALEOGEOGRAPHIC SETTING

Excellent outcrops of the Wenchang Formation are present in a roadcut in Tonglu County. These Ordovician rocks were deposited along the southeastern side of the Zhe-Wang Marginal Sea Basin, a part of the lower

JOURNAL OF SEDIMENTARY RESEARCH, VOL. 74, NO. 4, JULY, 2004, P. 527–536
 1527-1404/04/074-527/$03.00

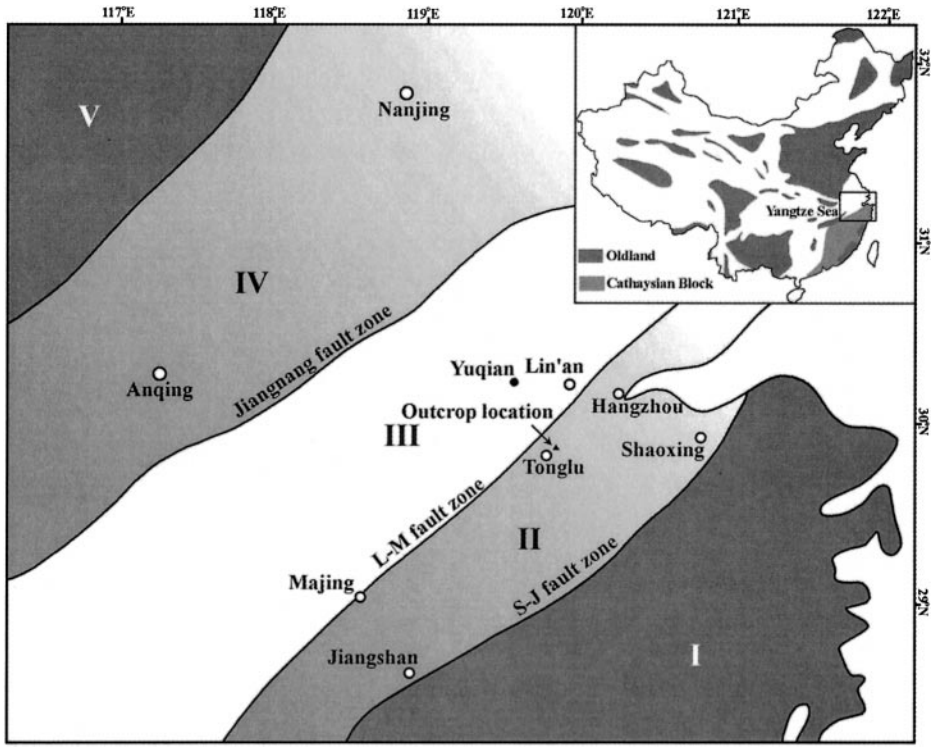

FIG. 1.—Paleogeography of the Zhe-Wang Marginal Sea Basin and location of the studied outcrop. Five paleogeographical units, bounded by faults, are identified: I, Cathaysian Block; II and IV, coastal (nearshore and shallow marine) zones; III, sub-deep sea; V, North China Oldland.

Paleozoic Yangtze Sea (Fig. 1). The Wenchang Formation is the youngest of three formations assigned to the Upper Ordovician Group, including the basal Huangnigang Formation and the Changwu Formation (Table 1). The Huangnigang Formation is composed of mudstone with calcareous concretions. Stratigraphic thickness changes from 72.7 m at the middle of the Jiangnang and Lin'an-Majing (L-M) fault zones to 22.0 m near the Shaoxing-Jiangshan (S-J) fault zone. The formation has been interpreted to represent a typical starved deep-sea facies (Yu 1996). Excellent outcrops of

TABLE 1.—*Stratigraphy of the Upper Ordovician in the Zhe-Wang Marginal Sea Basin.*

SYSTEM	SERIES	FORMATION	MEMBER	LITHOLOGY	DESCRIPTION	FACIES
ORDOVICIAN	UPPER ORDOVICIAN	Wenchang Fm.	Upper		Mud sandstone or sandy mudstone, with well-development of tidal bedding	Tidal-flat deposits
			Middle		Sandstone layers intercalated with two layers of conglomerate lenses	Nearshore sub-aqueous channel deposits
			Lower		Thick sandstone layer intercalated with thin mudstone layer, sandstone layers are massive or contain graded bedding and low-angle cross bedding	Nearshore and shallow-marine sandstone
		Changwu Fm.			Rhythmic alternation of mudstone layer and sandy siltstone layer, containing graptolites, gastropods, brachiopods, et al.	Deep-sea flysch to Shallow-marine flyschoid
		Huangnigang Fm.			Mudstone with calcareous concretions	Deep-sea mudstone

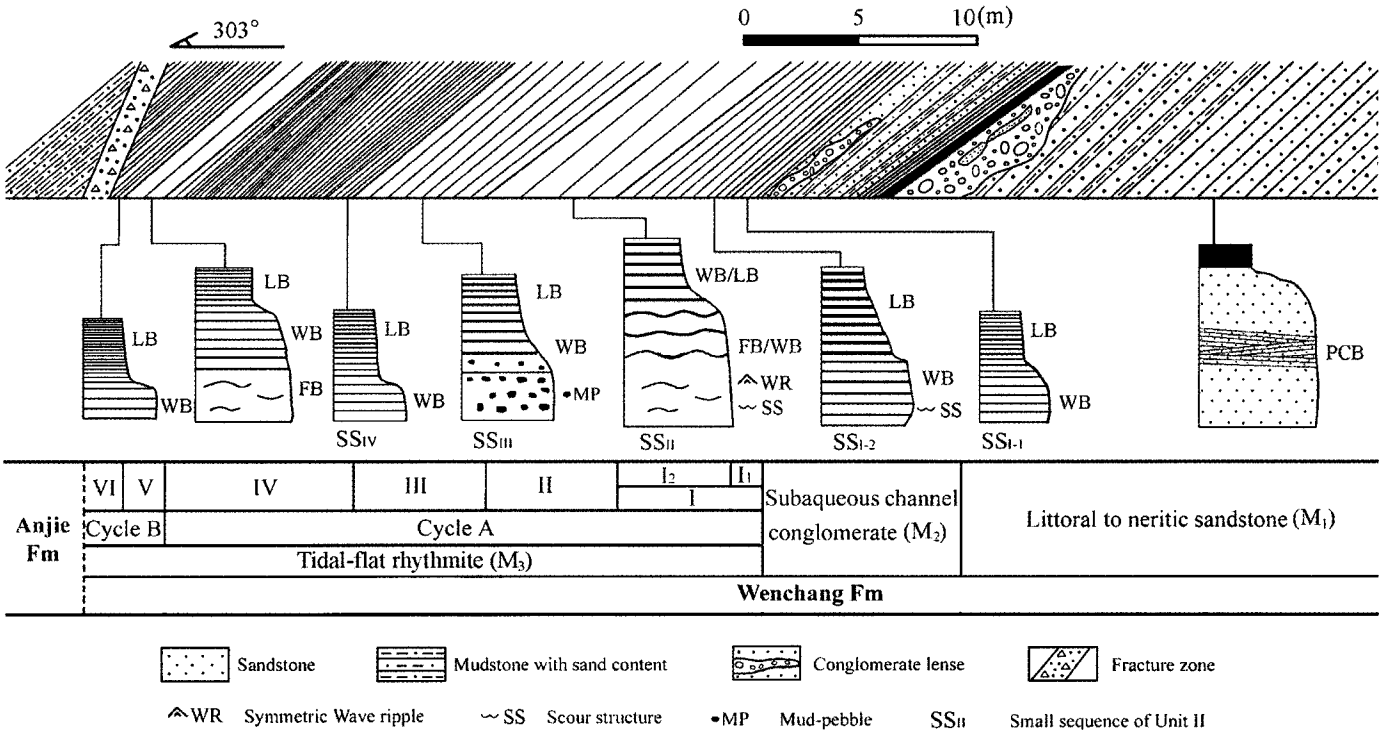

FIG. 2.—Lithological cross-section of the outcrop, the cyclic variation of sand lamina thickness, and the character of the small sequences. The Tonglu rhythmites are divided into Cycles A and B. PCB = low-angle planar cross bedding, LB = lenticular bedding, WB = wavy bedding, FB = flaser bedding, Anjie Fm = Anjie Formation, Wenchang Fm = Wenchang Formation.

the Changwu Formation is found at Yuqian (Fig. 1). The 1200-m-thick stratum is composed of 10,344 typical Bouma sequences with average individual sequence thickness of 11.8 cm (Luo 1990). The thickness of the Changwu Formation decreases from over 1200 m at the basin center to 320 m near the S-J fault zone. Along this transect, facies changes accordingly from typical deep-sea flysch into shallow-marine flyschoid that records uplifting and erosion of the active Cathaysian Block (Belt I in Fig. 1).

The Wenchang Formation is subdivided into three members (Table 1). The basal Wenchang member (M_1) is composed of medium to fine-grained yellowish and light-gray sandstone interbedded with dark gray mudstone. Sandstone layers are typically massive but occasionally display graded bedding and low-angle planar-cross bedding. Mudstone layers are horizontally bedded. Sandstone layers thin upward from 1.5 m to several centimeters, with a fining-upward trend. This fining-upward sandstone facies has a fossil assemblage of brachiopods, bryozoans, and crinoids, and was interpreted as shallow-marine to littoral deposits (Yu 1996; Fan 2001). The middle Wenchang member (M_2) consists of sandstone intercalated with conglomerate layers. The conglomerate layers are greenish gray, lenticular, and extend for more than 100 m (Fig. 2). The gravels and pebbles range from 0.5 to 18 cm in diameter with medium roundness and sphericity. The M_2 member is interpreted to be nearshore marine facies with the conglomerate layers representing ephemeral subaqueous channel deposits (Fan 2001). Lack of clast orientation is consistent with rapid sedimentation. The upper Wenchang member (M_3) is characterized by alternating light (sand-rich) and dark (mud-rich) laminae, commonly displaying lenticular, wavy, and flaser bedding. Raindrop imprints were observed on some bedding planes, indicating subaerial exposure. The M_3 member has been interpreted as tidal-flat deposits (Luo and Ge 1982; Fan 2001).

Facies analyses of the Upper Ordovician Group suggest a shallowing-upward progradational succession from deep-sea to coastal deposits (Table 1; Yu 1996; Fan 2001). Paleogeographic reconstruction suggests that the Cathaysian Orogenic Zone along the southeastern side of the basin started to be uplifted in the early Late Ordovician (Fig. 1). The orogenesis resulted in increased sedimentation and a gradual increase of the siliciclastic components (Table 1), as the basin infilled from the southeast. By the end of the Ordovician, the depocenter had crossed the S-J fault zone and was located between the L-M and the Jiangnan fault zones (Belt III, Fig. 1). Belt I, southeast of the S-J fault zone, was uplifted to be a part of the Cathaysian Block in the late Late Ordovician (Luo 1983; Zhou et al. 1993; Jin et al. 1998). The shoreline shifted between the S-J and the L-M fault zones (Belt II), where littoral to neritic sandstones were deposited (Fig. 2). The coast was geomorphologically ascribed to an open coast lacking barrier islands and/or bio-reefs (Luo and Ge 1982). Tonglu tidal flat is interpreted as an open-coast mesotidal flat with a spring tidal range of 4–5 m inferred from thickness of the intertidal deposits (Table 2). It is believed to be an ancient analogue of the modern tidal flats fringing the Yangtze delta, on the basis of the overall similar coast type of nonbarrier, the similar spring tidal range (4.6 m in the Changjiang Estuary), and the general lack of tidal-channel deposits (Fan 2001).

OUTCROP DESCRIPTION

A part of the basal Wenchang Formation, the middle and the upper Wenchang Fm, and the basal portion of the overlying lower Silurian Anjie Formation are well exposed along a roadcut near Tonglu county (Fig. 2). A 21-m-wide fracture zone separates the Wenchang and the Anjie formations.

Tonglu rhythmites show distinct thickness variations of sandy and muddy layers at both millimeter–centimeter and centimeter–decimeter scales. Individual sand or mud laminae range from less than 1 mm to several centimeters thick. In addition to the commonly observed millimeter–centimeter scale alternation of sand and mud laminae, a centimeter–decimeter scale alternation of sand-dominated and mud-dominated layers is apparent

TABLE 2.—*Statistics of sand/mud lamina thickness of different subfacies (thickness in millimeters).*

Sampling Sites									
Cycle	Unit	Subfacies	Bed Thickness	Total Couplet Number	Average Sand Lamina Thickness	Average Mud Lamina Thickness	Average Couplets Thickness	Ratios of Sand and Mud Lamina Thickness	Percent of Sand Laminae Thicker than 1 cm (%)
B	V	Lower intertidal	488	31	10.4	5.4	15.8	1.92	32.3
	IV	Upper intertidal	1376	218	2.6	3.7	6.3	0.69	0.9
	III	Middle intertidal	992	87	5.7	5.7	11.4	1.00	16.1
A	II	Lower intertidal	1939	111	11.5	6.0	17.5	1.91	35.1
	I	Subtidal	1867	157	5.4	6.4	11.8	0.84	14.6

(Fig. 3). Sand-dominated layers (SDLs) are characterized by sand laminae thicker than those in mud-dominated layers (MDLs). The number of sand–mud couplets in each SDL and MDL ranges from 9 to 22 pairs, with an average of 14.8 pairs. Thick sand laminae and SDLs can be traced laterally for tens of meters.

Two overall cycles of variation in sand-lamina thickness are distinguished in the Tonglu rhythmites (Fig. 2). Cycle A is composed of a thickening-upward succession followed by a thinning-upward succession, with the thickest laminae found in the middle. The total thickness of Cycle A is 6.2 m. The contact between Cycle B and the underlying Cycle A is abrupt. A thick sand lamina was found at the contact, followed by a thinning-upward trend. Cycle B is interpreted as a half cycle, comparable to the upper half of the Cycle A. The present study focuses on Cycle A because of better exposure, which permitted detailed measurements of the individual laminae. Cycle B is described qualitatively as comparative data for Cycle A.

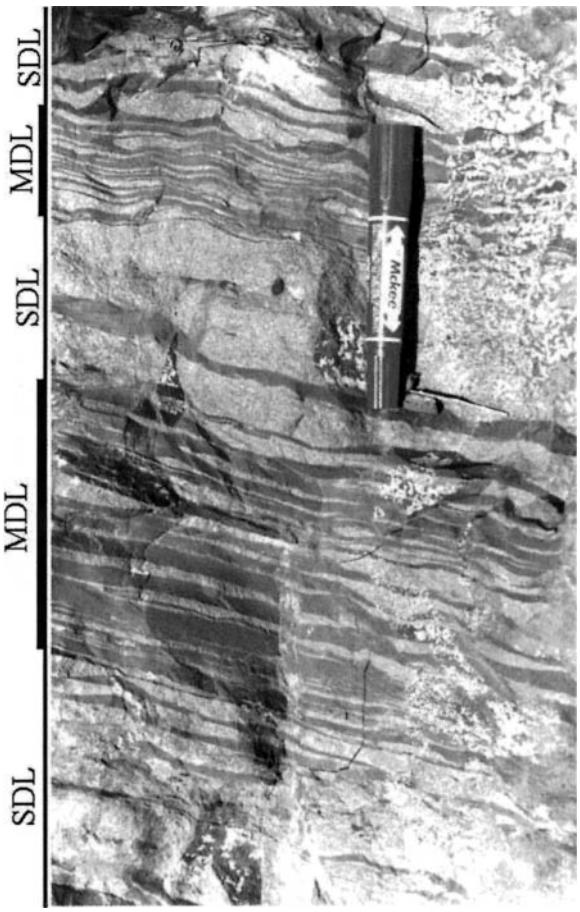

FIG. 3.—Alternating sand-dominated layers (SDLs) and mud-dominated layers (MDLs). Lithologically, a SDL is composed of muddy sandstone, and a MDL is composed of sandy mudstone. The pen is 12.6 cm long.

FACIES ANALYSIS

The Tonglu rhythmites are divided into six units: four in Cycle A and two in Cycle B (Fig. 2, Table 2). The different units are distinguished on the basis of the characteristics of the SDLs. The exact boundary between adjacent units is somewhat subjective.

Facies Description

Unit I is composed of gray sandy mudstone that displays a thickening-upward trend of sand-laminae thickness. Individual sand laminae are typically thinner than 20 mm, with an average of 5.4 mm (Table 2). This unit is further divided into Unit I_1 and Unit I_2 according to the variations of sedimentary structures and sand laminae thickness (Fig. 2). Unit I_1 is dominated by mudstone and lenticular bedding. Sand laminae are mostly thinner than 10 mm. Wavy bedding is common in the SDLs (SS_{I-1} in Fig. 2). Unit I_2 is composed of sandy mudstone and muddy sandstone. Most SDLs contain two or three layers of sand laminae of 10–20 mm thick. The SDLs display wavy bedding with occasional occurrence of flaser bedding (SS_{I-2} in Fig. 2). Erosional surfaces were observed at the bottom of some thick sand laminae (Fig. 4A).

Unit II consists of muddy sandstone and is characterized by the coarsest sediments, the thickest sand laminae, and the highest ratio of sand- and mud-lamina thickness in the entire cycle (Tables 2 and 3). The SDLs are typically composed of clusters of several thick ($>$ 10 mm) sand laminae. Flaser bedding, scour structures, symmetrical wave ripples, and asymmetrical ripples with diffused tops were observed in the SDLs (SS_{II} in Fig. 2; Fig. 4B, C, D). The asymmetrical ripples are also interpreted to be wave ripples by analogy with similar structures figured by Reineck and Singh (1980) and the associated symmetrical wave ripples.

Unit III consists of sandy mudstone. The most distinctive feature is that the thick sand laminae in the SDLs are studded with mud pebbles (SS_{III} in Fig. 2; Fig. 4E). The mud pebbles share identical lithological characteristics with the mud laminae. Most of the mud pebbles are 5 mm to 8 mm in diameter with a maximum of 18 mm. Their shapes change from angular to subrounded (Fig. 4F). The subrounded pebbles tend to be isolated in the sand laminae, whereas the angular pebbles tend to be aligned parallel to the mud laminae. It is apparent that the mud pebbles are intraformational, originated from the adjacent consolidated (but not lithified) mud laminae, probably owing to erosion by waves or currents. Unit III demonstrates a fining-upward sequence. Silt content in the sand laminae is low, and grain-size distribution is bimodal (Table 3).

Unit IV is composed of dark-gray mudstone with well-developed lenticular bedding (SS_{IV} in Fig. 2). The lateral extent of the sand laminae is poor. Most of the sand laminae are thinner than 10 mm. The unit has the finest sediments, the thinnest sand laminae, and the lowest ratio of sand- and mud-lamina thickness in the entire cycle (Table 2).

Unit V consists of muddy sandstone. Several thick sand laminae ($>$ 10 mm) cluster to form the SDLs like those in Unit II (SS_v vs. SS_{II} in

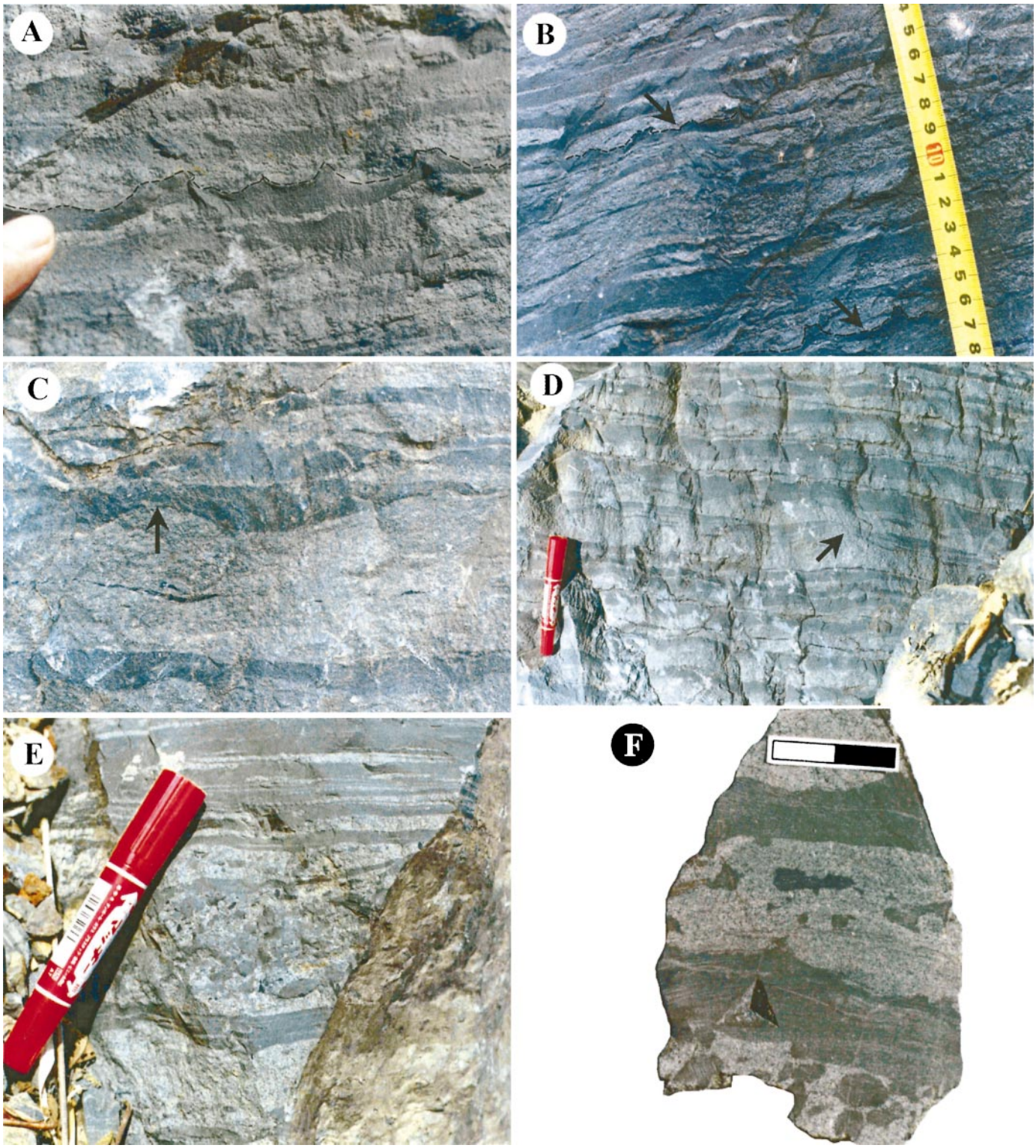

FIG. 4.—Sedimentary structures: **A)** Scour structures (dashed line at finger), upper part of the subtidal zone (Unit I_2 in Figure 2). **B)** Flaser bedding and scour structures (dashed line at arrows), SDL in the lower intertidal zone (Unit II), scale in centimeters. **C)** Thick sand lamina with symmetrical wave ripples at the top and flaser mud laminae, lower intertidal zone. **D)** Asymmetrical wave ripples with diffuse top, lower intertidal zone. The pen is 12.6 cm long. **E)** Thick sand laminae studded with mud pebbles, SDLs in the middle intertidal zone (Unit III). **F)** Mud pebbles in angular, subangular or subrounded shapes, middle intertidal zone (Unit III). Scale bar is in centimeters.

TABLE 3.—*Grain-size data from sand layers in the Tonglu rhythmites.*

Sample number	Sampling site	Grain-size component (%)			Mean grain size Mz (ϕ)	Standard deviation (σ_1)
		Sand	Silt	Clay		
5		33.78	6.22	60.00	6.8	2.8
4	Unit III	54.88	0.12	45.00	4.9	2.9
3		59.85	0.15	40.00	4.8	2.9
2	Unit II	62.61	22.39	15.00	4.0	1.4
1		43.26	41.74	15.00	4.2	1.3

Fig. 2). Erosional surfaces are common at the bottom of the thick sand laminae. Thickness of sand laminae ranges from 1 mm to 42 mm with an average of 10.4 mm (Table 2).

Unit VI is composed of muddy sandstone and sandy mudstone with a fining-upward sequence. In this unit, wavy and lenticular bedding is common. The thickness of individual laminae, however, could not be measured accurately because of the degraded exposure.

Facies Interpretation

Cycle A (units I through IV) consists of a coarsening-upward sequence followed by a fining-upward sequence. The coarsening- to fining-upward trend is caused by the variation of the sand-lamina thickness, in addition to the size of the grains (Table 2, 3). This trend bears considerable resemblance to the modern open-coast tidal-flat sequence along the Yangtze delta, where coarser sediments and thicker sand laminae tend to be deposited on the lower intertidal zone, and sediment grain size, as well as the thickness of sand laminae, decreases both landward and seaward from the lower intertidal zone (Li and Wang 1998). On the basis of the analog of the modern Yangtze tidal flat, Unit I is interpreted to be subtidal facies with a coarsening-upward sequence. Units II, III, and IV are interpreted to be lower, middle, and upper intertidal facies, respectively. The raindrop imprints and intraformational mud pebbles in Unit III support the interpretation of a middle intertidal origin. The subrounded mud pebbles were also observed in erosional hollows in the middle intertidal flats at the Yangtze tidal flat (Li and Wang 1998).

Lithology, sedimentary structures, and the lamina thickness of Unit V are nearly identical to those of Unit II (Table 2). Unit V is thus interpreted to be the lower intertidal facies for Cycle B. The overlying Unit VI with thinner sand laminae is interpreted to be middle-upper intertidal facies.

There is no field evidence suggesting that any part of Units I through VI are associated with tidal channels. Laterally migrated foresets are absent, and all of the units exhibit conformable contacts with the strata that underlie them. The possibility of tidal channels can also be excluded on the basis of the fine-scale vertical accumulation of laminae and the lateral extent of sand laminae and SDL over many tens of meters.

PERIODICITIES IN THE TONGLU RHYTHMITES AND THEIR INTERPRETATION

Periodicities of Sand-Lamina Thickness Variation

In order to minimize uncertainties in the lamina-thickness measurements due to ripple forms and variations in lateral extent, the sand-lamina thicknesses in Cycle A were smoothed using a three-point moving average (Fig. 5A). Discrete Fourier analysis of the smoothed data indicates a peak period of 13.5 laminae (Fig. 5B), with secondary peaks at 64.0, 34.1, 25.6, and 17.7 laminae. A broad peak also occurred between 8 and 12 laminae. It is worth noting that the 13.5-lamina peak is roughly half of the 25.6-lamina peak, which is roughly half of the 64-lamina peak. The peak period of 13.5 laminae is also close to the averaged number of sand laminae of 14.8 per small sequence, i.e., the sand- and mud-dominated layer, in Cycle A.

The Neap–Spring Tide Interpretation of the Periodicities

Cyclic variation of sand-lamina thickness has been explained by neap–spring tidal variations whereby thick laminae correspond to spring tides and thin laminae correspond to neap tides (e.g., Visser 1980; Allen 1981; Kvale et al. 1989; Archer 1994; Greb and Archer 1995; Williams 1998; Eriksson and Simpson 2000). Therefore, the rhythmic alternations of SDLs and MDLs may represent the fortnightly cycles of spring and neap tides. Adopting the above concept, the peak period of 13.5 laminae in the Tonglu rhythmites may reflect the neap–spring tidal cycle, and secondary periods of 25.6 and 64 laminae may reflect monthly and bimonthly cycles. A two-month cycle has also been reported in a study of modern tidal rhythmites in Muir Inlet, Alaska (Cowan et al. 1998).

The entire Cycle A is 6.17 m thick and contains a total of 573 couplets (Table 2). On the basis of a neap–spring interpretation, it would require 42.4 semimonthly neap–spring cycles to deposit the 573 couplets (573 couplets at 13.5 couplets per cycle). Such analysis suggests that the entire Cycle A was deposited in 1.8 years at a sedimentation rate of 3.43 m/yr. A wide range of sedimentation rates, from 0.03 to 12.5 m/yr, has been reported for ancient and modern tidal rhythmites (Table 4), mostly on the basis of the above logic of analyses. Rhythmites recording high rate of sedimentation have been interpreted as filling available accommodation space with abundant sediment supply.

Tidal channels are areas where rapid and continuous sedimentation can occur in a short period of time. The highest sedimentation rates often reflect channel migration rather than vertical accretion. Although many modern tidal rhythmites studies have been conducted in migrating tidal channels (e.g., Visser 1980; Allen and Homewood 1984; Yang and Nio 1985), Dalrymple et al. (1991) pointed out that migrating channels are also sites of erosion. The net vertical sedimentation rate may, therefore, be negligible despite anomalously high local rates of ''horizontal'' sedimentation. In contrast, tidal flats are usually considered as unsteady accretion environments with relatively slow vertical aggradation (Anderson et al. 1981). Few modern tidal rhythmites have been documented on the intertidal flats, and most of these examples are located at the inner part of macrotidal estuaries like the Bay of Fundy (Dalrymple et al. 1991), the Mont-Saint-Michel Bay (Tessier 1993), and the Turnagain Arm estuary (Atwater et al. 2001). In the last case, the accommodation space was created by tectonic subsidence in the 1964 Alaska earthquake (Atwater et al. 2001). These rhythmites of high sedimentation rates are limited in temporal and spatial extent, with a thickest section of 1.8 m. Ancient rhythmite sections range in thickness from several meters to tens of meters. Their continuity and high sedimentation rates have been questioned by Fan and Li (2002), who argue that the unstable dynamic environment of tidal flats and variation of sedimentation rates over different time scales do not favor long-lasting high rates of sedimentation.

In the case of the Tonglu rhythmites, the 3.43 m/yr sediment rate implied by the neap–spring tidal cycle interpretation is extremely high. Furthermore, such a rate does not account for compaction during burial and diagenesis. It is reasonable that high rates of rhythmite sedimentation exist for short time frames, and occur only where there is abundant sediment supply and rapid creation of accommodation space. The creation of accom-

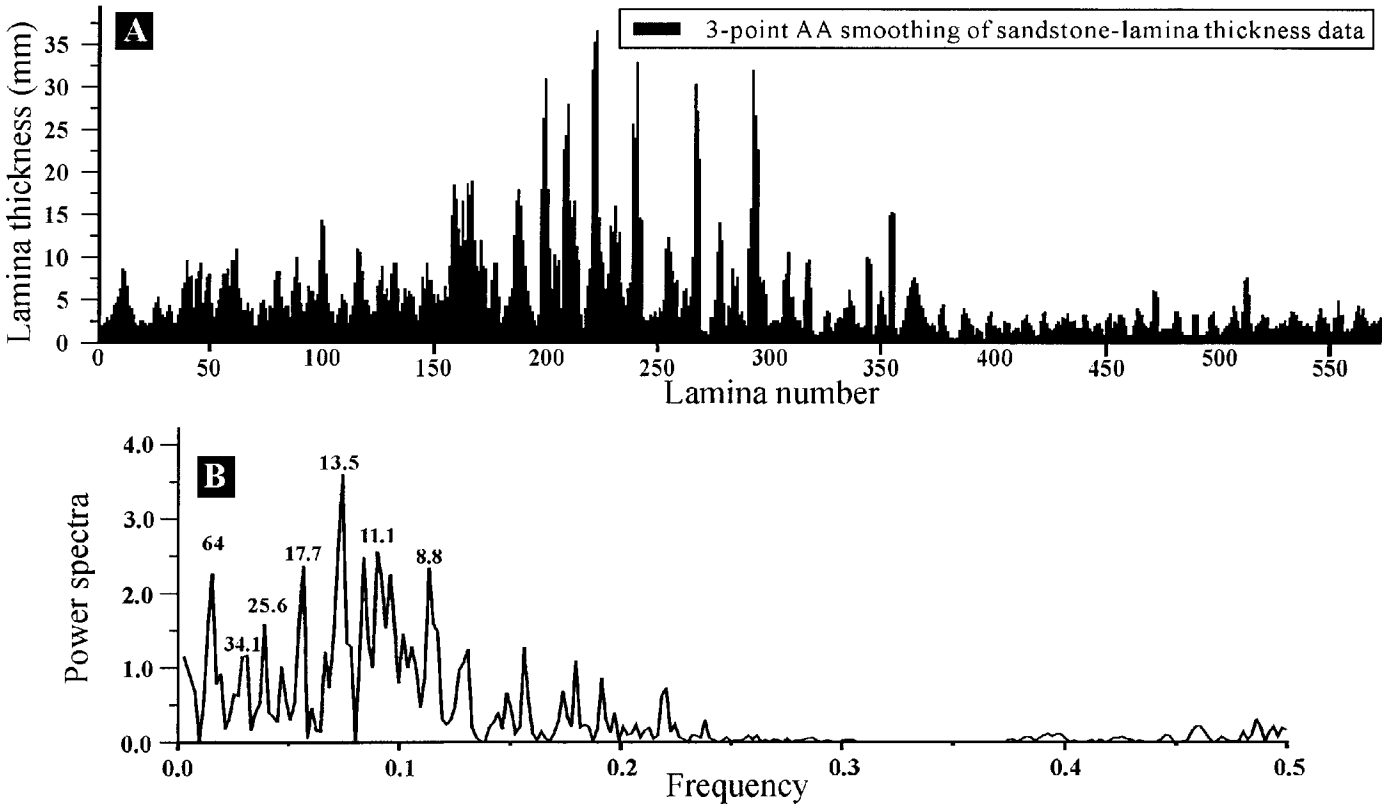

FIG. 5.—Lamina-thickness variations in Cycle A: **A)** 3-point averaged sand-lamina thickness; **B)** frequency distribution of the thickness variation.

modation space must approximately match the sedimentation rate in order to maintain the subtidal–intertidal depositional environment. Too fast or too slow creation of accommodation space would result in changes of depositional environment.

No reliable evidence has been found to indicate possible mechanisms of abundant sediment supply and rapid creation of accommodation space in the Tonglu area supporting the high sedimentation rate of 3.43 m/yr. On a regional scale, the Tonglu area was believed to undergo tectonic uplift instead of subsidence in the Late Ordovician (Yu 1996; Fan 2001). The general lack of tidal channels and the overall horizontal strata eliminate the possibilities of ''horizontal'' accumulation from channel migration. Both the above analyses cast a doubt on the neap–spring tidal cycle interpretation of the Tonglu rhythmites. In the following, we attempt an alternative interpretation.

Influence of Storm Erosion and Deposition on the Rhythmites

The presence of symmetrical wave ripples at tops of the relatively thick sand laminae in the SDLs toward the lower intertidal facies suggests considerable wave influence. Erosional surfaces beneath many sand laminae within the SDLs indicate that fine-scale (possibly daily, weekly, or monthly) erosional hiatuses can not be neglected. Conditions for the formation and preservation of continuous tidal rhythmites in wave-protected environments, such as semi-enclosed estuaries (Dalrymple et al. 1991; Shi 1991; Tessier 1993) may not apply in the Tonglu rhythmites. Wave-induced accumulation and erosion may not be negligible and should be incorporated in the interpretation.

The intraformational mud pebbles observed in some of the thick sand laminae are interpreted to be erosional features caused by waves and currents instead of desiccation features. The subrounded mud pebbles tend to be ''floating'' within sandstone layers, suggesting that they might have been suspended before deposition. We believe that this results from storm-wave action instead of tidal currents. The bimodal distribution of grain size and the high standard deviation (poor sorting) in the sand laminae with mud pebbles (Unit III in Table 3) indicates that sandy and clayey grains and mud pebbles should have been suspended during high-energy periods and settled quickly out of the highly turbulent water body with less grading during storm-waning periods.

TABLE 4.—*Comparison of estimated sedimentation rates based on neap-spring cyclicity.*

Sedimentation rate ($m\ yr^{-1}$)	Origin	Where tidal rhythmites developed	Ages of tidal rhythmites
3.43	This paper	Zhe-wang marginal basin, China	Late Ordovician
0.03–0.6	Miller and Erikson (1997)	Appalachian Basin, USA	Early Carboniferous
3.8	Lanier et al. (1993)	Western Interior Coal Basin, USA	Late Carboniferous
0.91–1.32	Martino and Sanderson (1993)	Appalachian Basin, USA	Early Carboniferous
7.0	Dalrymple et al. (1991)	Bay of Fundy, Canada	Modern
1.0	Kuecher et al. (1990)	Illinois Basin, USA	Late Carboniferous
0.75–12.5	Kvale and Archer (1990)	Illinois Basin, USA	Late Carboniferous
0.35	Brown et al. (1989)	Illinois Basin, USA	Early Carboniferous
1.1	Kvale et al. (1989)	Illinois Basin, USA	Late Carboniferous
12	Tessier and Gigot (1989)	Digne Basin, France	Miocene

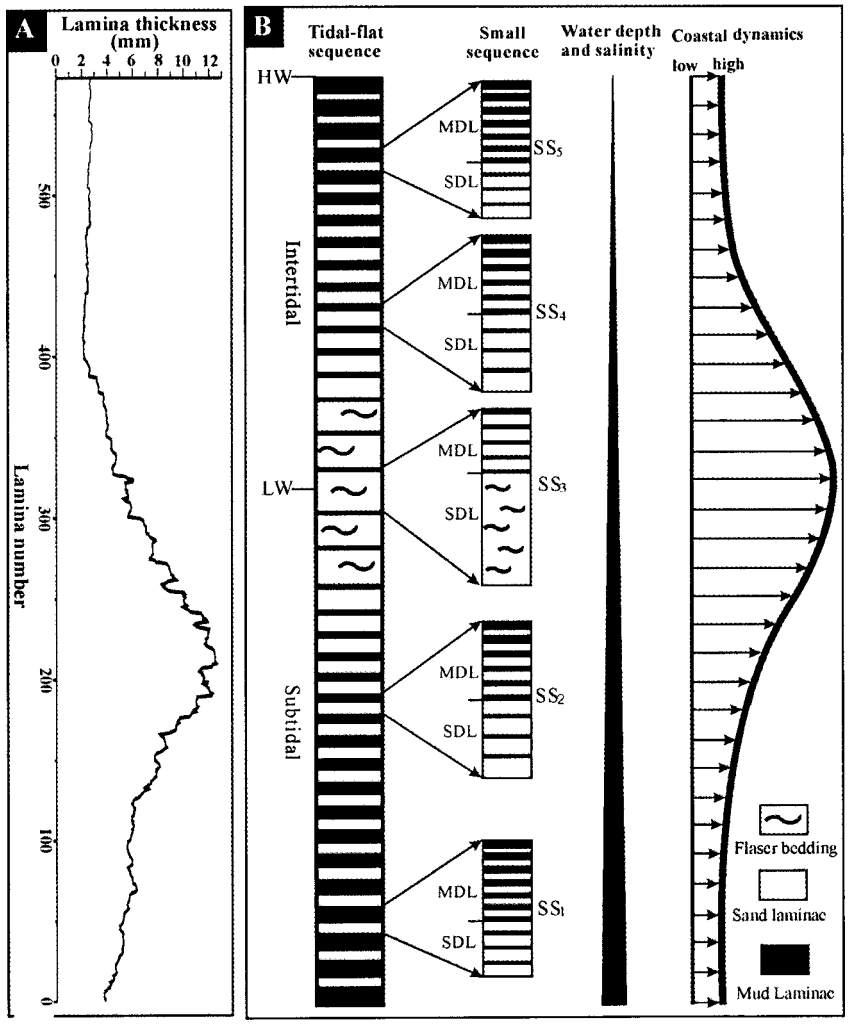

FIG. 6.—**A)** Variation of 64-point averaged sand lamina thickness. **B)** Schematic vertical successions of tidal-flat deposits, including both subtidal and intertidal zones (modified after Li et al. 1992).

A thick sand lamina is often found at the bottom of the sand-dominated layers with abrupt contact with underlying layers. The thick sand laminae at the bases of many SDLs are often characterized by a bottom erosional surface, symmetrical wave ripples at the top, and the presence of mud pebbles. We suggest that these thick sand laminae represent deposition during the waning phase of storms. A similar storm interpretation on the formation of sand-dominated layers was suggested by Li et al. (2000) at a modern open-coast tidal flat fringing the Yangtze delta, while the mud-dominated layers, composed of the alternation of thin sand and mud laminae, were deposited during normal weather conditions. Another modern analog was provided by van den Berg (1981) who linked the coarse thick layers with winter (high wave) deposits and the fine thin layers with summer (low wave) deposits in a mesotidal channel fill sequence at Oosterschelde Mouth, The Netherlands. Bhattacharyya et al. (1980) documented similar patterns of storm and calm weather depositions in the intertidal upper Proterozoic Lower Bhander Sandstone around Maihar, Satna district, Madhya Pradesh, India.

The present interpretation of storm and calm weather depositions does not explain the 13.5 layer periodicity of the Tonglu rhythmites. The average number of couplets in each small sequence of the Tonglu rhythmites is 14.8 but varies in a wide range from 9 to 22. Similar random variation of the couplet number in each small sequence was documented in the Yangtze tidal flat, where 16–26 couplets were identified (Fan et al. 2002). Although the peak periodicity obtained from statistical analyses agrees with the neap–spring tidal cyclicity, our detailed observation did indicate considerable variation in couplet numbers.

Although individual wave events occur randomly, seasonal alteration of calm- and rough-weather deposits should occur quasi-regularly. Seasonal variations on tidal flats of bed level, morphology, and composition have been widely documented (e.g., O'Brien et al. 2000; Healy et al. 2002). We thus interpret the 13.5 layer periodicity of the Tonglu rhythmites to this seasonal alteration of tidal-flat dynamics, with the evidence indicating that erosion caused by high-energy storm events played a significant role.

STORM-RELATED TIDAL-FLAT SUCCESSION AND ITS IMPLICATION

Subtidal to Intertidal Succession

The relatively thick sand laminae and sand-dominated layers tend to be the thickest in the succession interpreted as lower intertidal facies (Fig. 2, Table 2). Similar trends were observed on a modern tidal flat by Li et al. (1992), as shown in Figure 6B. Examining Figures 2 and 6B, it is evident that the tidal bedding and the trends of the small sequences are quite comparable between the Tonglu rhythmites and the modern Yangtze tidal flat. Flaser bedding dominates the lower intertidal facies (SS_{II} vs. SS_3). Wavy bedding dominates in both the middle intertidal zone and the upper subtidal zone (SS_{III} vs. SS_4, $SS_{I\text{-}2}$ vs. SS_2), whereas lenticular bedding is the dominant sedimentary structure in the upper intertidal zone and the lower subtidal zone (SS_{IV} with SS_5, $SS_{I\text{-}1}$ with SS_1).

Reineck and Gerdes (1997) described a similar cross-shore distribution pattern of storm sand layers (similar to the SDL here) in a subtidal–intertidal environment along the southern North Sea coast. In the subtidal zone, thin storm sand layers are intercalated with the shelf mud. Towards the low-water line, the thickness of the storm sand layers increases and reaches the maximum at around the low-water line. In the intertidal zone, the storm sand layers are intercalated with muddy tidal-flat sediments and gradually decrease in thickness towards the high-water line (Reineck and Gerdes 1997). This lateral variation in thickness of storm sand layers is related to the cross-shore distribution patterns of the relative energy levels of wave and current and to frequencies of submergence and emergence of a tidal flat (Reineck and Gerdes 1997).

The data on sand-lamina thickness across Cycle A of the Tonglu rhythmites were smoothed with a 64-point moving average, where 64 represents the longest period identified by the time-series analysis (Fig. 5). The smoothed curve matches well with the schematic trend of coastal dynamics established by Li et al. (1992) and Reineck and Gerdes (1997) (Fig. 6). The variations in thickness of tidal laminae and sand-dominated layers are controlled by the cross-shore evolution of the depositional environment instead of individual tides.

Sedimentation Rate and Preservation Potential

As discussed above, the extremely high sedimentation rate of 3.43 m/yr obtained from the lamina counting and neap–spring tide interpretation could not be justified in terms of sediment supply and creation of accommodation space. On the basis of studies at a modern open-coast tidal flat fringing the Yangtze delta, Fan et al. (2002) suggested a preservation potential of 33.3% for the small sequences (representing one-year interval), and Li et al. (2000) suggested a 0.2% preservation potential for individual lamina. If the 33.3% preservation potential is applied to the Tonglu rhythmites, the 42.4 small sequences counted from the outcrop would represent 127.3 years of deposition. A sedimentation rate of 4.8 cm/yr is obtained (617.4 cm over 127.3 years).

The 6.17 m thick Cycle A contains 573 sand- and mud-lamina couplets. It is generally accepted that four laminae can theoretically be deposited during one tidal cycle (e.g., Li et al. 1965; Allen 1985). Under a typical semidiurnal tidal regime, there are 70,645 tidal cycles in 100 years. Thus, 282,580 laminae, or 141,290 couplets, could be deposited. With a 0.2% preservation potential (Li et al. 2000), 283 couplets would be preserved during a period of 100 years. Therefore, the measured 573 couplets in Cycle A would represent 202 years of deposition at a sedimentation rate of 3 cm/yr. This is similar to the 4.8 cm/yr sedimentation rate obtained based on Fan et al. (2002). A sedimentation rate of 3–5 cm/yr is comparable to the 4.2 cm/yr rate at the modern tidal-flat fringing the Yangtze delta.

The modern sedimentation rate and preservation potential were deduced over a centennial scale from a tidal flat with tremendous suspended-sediment supply (from the Yangtze River) under a relatively stable seal level. Both Li et al. (2000) and Fan et al. (2002) found that preservation potential decreases with increasing temporal scales. Therefore, the sedimentation rate of Cycle A might be lower than the 3 to 5 cm/yr because its estimated depositional time was longer than one hundred years. Moreover, the erosional surface between Cycles A and B could represent a long hiatus.

Significance of Storm-Related Tidal-Flat Rhythmites

Tonglu storm deposits developed in an open-coast tidal-flat environment. The preservation potential of storm-generated structures is usually considered to be low in such environments because of intense bioturbation and reworking by waves and tides (Duke 1985; Reineck and Gerdes 1997). Modern analogues have been identified in the Yangtze Delta, where tidal flats accumulate approximately 4 cm per year (Li et al. 2000; Fan and Li 2002). Rapid sedimentation on the Tonglu tidal flats may stem from enhanced sediment supply from the rapidly rising Cathaysian orogenic zones. These case studies indicate that storm deposits can be well preserved at open-coast tidal flats given that local deposition rate is high.

Both tides and storm waves are effective agents for sediment transportation in shallow marine and nearshore settings. However, many ancient shallow-marine depositional systems are interpreted as either being storm-wave-dominated or tide-dominated (Prave et al. 1996). In this paper, the second-order alternations of sand-dominated layers and mud-dominated layers are interpreted to be caused by storm and calm weather alternations. In other words, the Tonglu tidal flats, similar to modern tidal flats fringing the Changjiang Delta, demonstrate variations of storm-wave-dominated seasons and calm tide-dominated seasons.

Although studies on wave-induced sediment transport are often focused on beach and shoreface environments, wave forcing is often neglected on tidal flats. Cycle A, a complete subtidal–intertidal flat succession, provides a case study of wave deformation and sediment transportation during storms. Vertical variation of parameters such as grain size, thickness of the SDLs, and sand-lamina thickness (see Table 2) are useful data to understand cross-shore evolution of storm wave energy and sediment transport processes.

CONCLUSIONS

Tonglu rhythmites, composed of sand- and mud-lamina couplets, display vertical grouping of sand- and mud-dominated layers. The sand-dominated layers are characterized by the presence of relatively thick sand laminae, erosion surfaces, mud pebbles, and oscillation ripples, and are interpreted as wave-influenced storm deposits. The mud-dominated layers are interpreted as calm-weather deposits reflecting tidal forcing.

One complete and one partial thickening–thinning cycle, was identified in outcrop. Comparison of these cycles to modern tidal-flat facies suggests consistency with combined tide and wave processes in the subtidal–intertidal environment. Variation of sand-lamina thickness in the 6.2-m-thick Cycle A is believed to be related to energy variation in the subtidal–intertidal zone rather than to individual tidal cycles.

Time-series analysis of sand-lamina thickness variation revealed a peak period of approximately 14 laminae, with minor peaks occurring at 26 and 64 laminae. Although the 14-layer peak coincides with the neap–spring tidal cycles identified in other rhythmites, neap–spring variation is rejected here because of the requirement of an unrealistically high sedimentation rate of 3.43 m/yr. We suggested an alternative interpretation in which the thick sand laminae are related to storm deposition on the basis of erosional surfaces, mud pebbles, and oscillatory wave ripples in the thick sand laminae. Our interpretation is also based on the regional paleogeography and comparison with the modern Yangtze tidal flat. Applying the results of Li et al. (2000) and Fan et al. (2002) from the Yangtze open-coast tidal flat, a sedimentation rate of 3 cm/yr was obtained for the Tonglu rhythmites.

Storm waves act not only as destructive agents to calm-weather deposition but also as efficient agents for sediment transport and deposition. Alternations of the sand-dominated layers and the mud-dominated layers suggest that the tidal flats changed seasonally from tide-dominated to storm-wave-dominated. Vertical variations in grain size and thickness of sand laminae and sand-dominated layers are indicators of cross-shore changes of storm energy and sediment transport processes.

ACKNOWLEDGMENTS

This research was supported by the National Natural Science Foundation of China (grant no. 40176022, 40046019). We thank Prof. Luo Zhang, Dr. Deng Bing, Dr. Cai Jingong, and Mr. Li Tiesong for their assistance in the fieldwork. We also thank Dr. A.W. Archer for his insightful discussion on the origin of the Tonglu rhythmites in the field. We greatly appreciate the critical and constructive reviews provided by Drs. Erik Kvale, Daniel Miller, and one anonymous reviewer.

REFERENCES

ALLEN, J.R.L., 1981, Lower Cretaceous tides revealed by cross-bedding with mud drapes: Nature, v. 289, p. 579–581.

ALLEN, J.R.L., 1985, Principles of Physical Sedimentology: London, George Allen & Unwin, 267 p.

ALLEN, J.R.L., AND DUFFY, M.J., 1998, Temporal and spatial depositional patterns in the Severn Estuary, southwestern Britain: intertidal studies at spring–neap and seasonal scales, 1991–1993: Marine Geology, v. 146, p. 147–171.

ALLEN, J.R.L., AND HOMEWOOD, P., 1984, Evolution and mechanics of a Miocene tidal sandwave: Sedimentology, v. 31, p. 63–81.

ANDERSON, F.E., BLACK, L., WATLING, L.E., MOOK, W., AND MAYER, L.M., 1981, A temporal and spatial study of mudflat erosion and deposition: Journal of Sedimentary Petrology, v. 51, p. 729–736.

ARCHER, A.W., 1994, Extraction of sedimentological information via computer-based image analyses of gray shales in Carboniferous coal-bearing sections of Indiana and Kansas, U.S.A.: Mathematical Geology, v. 26, p. 47–65.

ARCHER, A.W., AND JOHNSON, T.W., 1997, Modeling of cyclic tidal rhythmites (Carboniferous of Indiana and Kansas, Precambrian of Utah, U.S.A.) as a basis for reconstruction of intertidal positioning and palaeotidal regimes: Sedimentology, v. 44, p. 991–1010.

ATWATER, B.F., YAMAGUCHI, D.K., BONDEVIK, S., BARNHARDTT, W.A., AMIDON, L.J., BENSON, B.E., SKJERDAL, G., SHULENE, J.A., AND NANAYAMA, F., 2001, Rapid resetting of an estuarine recorder of the 1964 Alaska earthquake: Geological Society of American Bulletin, v. 113, p. 1193–1204.

BHATTACHARYYA, A., SARKAR, S., AND CHANDA, S.K., 1980, Storm deposits in the late Proterozoic lower Bhander sandstone of Vindhyan supergroup around Maihar, Satna district, Madhya Pradesh, India: Journal of Sedimentary Petrology, v. 50, p. 1327–1336.

BROWN, M.A., ARCHER, A., AND KVALE, E.P., 1990, Neap–spring cyclicity in laminated carbonate channel-fill deposits and its implications: Salem limestone (Mississippian), south-central Indiana, U.S.A: Journal of Sedimentary Petrology, v. 60, p. 152–159.

COWAN, E.A., CAI, J., POWELL, R.D., SERAMUR, K.C., AND SPURGEON, V.L., 1998, Modern tidal rhythmites deposited in a deep-water estuary: Geo-Marine Letters, v. 18, p. 40–48.

DALRYMPLE, R.W., MAKINO, Y., AND ZAITLIN, B.A., 1991, Temporal and spatial patterns of rhythmite deposition on mud flats in the macrotidal Cobequid Bay–Salmon River estuary, Bay of Fundy, Canada, *in* Smith, D.G., Reinson, G.E., Zaitlin, B.A. and Rahmani, R.A., eds., Clastic Tidal Sedimentology: Canadian Society of Petroleum Geologist, Memoir 16, p. 137–160.

DUKE, W.L., 1985, Hummocky cross-stratification, tropical hurricanes, and intense winter storms: Sedimentology, v. 32, p. 167–194.

ERIKSSON, K.A., AND SIMPSON, E.L., 2000, Quantifying the oldest tidal record: the 3.2 Ga Moodies Group, Barberton Greenstone Belt, South Africa: Geology, v. 28, p. 831–834.

FAN, D.D., 2001, Formation and preservation of rhythmic deposition on mudflat and quantitative analysis of diastems [unpublished Ph.D. thesis]: Tongji University, Shanghai, 107 p. (in Chinese with English abstract).

FAN, D.D., AND LI, C.X., 2002, Rhythmic deposition on mudflats in the mesotidal Changjiang estuary, China: Journal of Sedimentary Research, v. 72 p. 543–551.

FAN, D.D., LI, C.X., ARCHER, A.W., AND, WANG, P., 2002, Temporal distribution of diastems in deposits of an open-coast tidal-flat with high suspended sediment concentrations: Sedimentary Geology, v. 152, p. 173–181.

GREB, S.F., AND ARCHER, A.W., 1995, Rhythmic sedimentation in a mixed tide and wave deposit, Hazel Patch Sandstone (Pennsylvanian), Eastern Kentucky coal field: Journal of Sedimentary Research: v. 65B, p. 96–106.

HEALY, T., WANG, Y., AND HEALY, J.A., EDS., 2002, Muddy Coasts of the World: Process, Deposits and Function: Amsterdam, Elsevier, 542 p.

JIN, W.S., ZHAO, F.Q., AND ZHANG, H.M., 1998, Division of tectonic units and its characteristics: Zhejiang Geology, v. 14, p. 1–10 (in Chinese with English abstract).

KLEIN, G. DEV., 1975, Epilogue, tidal sedimentation: some remaining problems, *in* Ginsburg, R.N., ed., Tidal Deposits: A Casebook of Recent Examples and Fossil Counterparts: Berlin, Springer-Verlag, p. 407–510.

KUECHER, G.J., WOODLAND, B.G., AND BROADHURST, F.M., 1990, Evidence of deposition from individual tides and of tidal cycles from the Francis Creek Shale (host rock to the Mazon Creek Biota), Westphalian D (Pennsylvanian), northeastern Illinois: Sedimentary Geology, v. 68, p. 211–221.

KVALE, E.P., AND ARCHER, A.W., 1990, Tidal deposits associated with low-sulfur coals, Brazil Formation (Lower Pennsylvanian), Indiana: Journal of Sedimentary Petrology, v. 60, p. 563–574.

KVALE, E.P., ARCHER, A.W., AND JOHNSON, H.R., 1989, Daily, monthly, and yearly tidal cycles within laminated siltstones of the Mansfield Formation of Indiana: Geology, v. 17, p. 365–368.

KVALE, E.P., JOHNSON, H.W., SONETT, C.P., ARCHER, A.W., AND ZAWISTOSKI, A., 1999, Calculating lunar retreat rates using tidal rhythmites: Journal of Sedimentary Research, v. 69, p. 1154–1168.

LANIER, W.P., FELDMAN, H.R., AND ARCHER, A.W., 1993, Tidal sedimentation from a fluvial to estuarine transition, Douglas Group, Missourian–Virgilian, Kansas: Journal of Sedimentary Petrology, v. 63, p. 860–873.

LI, C.X., AND WANG, P.X., 1998, Late Quaternary stratigraphy of the Yangtze Delta: Beijing, China Science Press, 222 p. (in Chinese).

LI, C.X., HAN, C.P., AND WANG, P., 1992, Deposition sequences and storm deposition on low-energy coast of China: Acta Sedimentologia Sinica, v. 13, p. 119–128 (in Chinese with English abstract).

LI, C.X., WANG, P., FAN, D.D., DENG B., AND LI, T.S., 2000, Open-coast intertidal deposits and the preservation potential of individual lamina: a case study from East-central China: Sedimentology, v. 47, p. 1039–1051.

LI, C.X., YANG, X., ZHUAN, Z., JIAN, Q., AND WU, S., 1965, Formation and evolution of the intertidal mudflat: Journal, Shangdong College of Oceanography, v. 2, p. 21–31 (in Chinese with English abstract).

LUO, Z., 1983, Tectonic systems in Zhejiang Province: Technical Report of the Petroleum Institute of Zhejiang, no. 8306, 22 p. (in Chinese).

LUO, Z., 1990, Upper Ordovician turbidite in Yuqian County, Zhejiang Province: Zhejiang Geology, v. 6, p. 20–29 (in Chinese with English abstract).

LUO, Z., AND GE, H.H., 1982, Sedimentary environment and facies of the Upper Sinian and Lower Paleozoic in Zhejiang Province, China: Zhejiang Petroleum Geology, v. 9, p. 12–17 (in Chinese with English abstract).

MARTINO, R.L., AND SANDERSON, D.D., 1993, Fourier and autocorrelation analysis of estuarine tidal rhythmites, lower Breathitt Formation (Pennsylvanian), eastern Kentucky, U.S.A.: Journal of Sedimentary Petrology, v. 63, p. 105–119.

MILLER, D.J., AND ERIKSSON, K.A., 1997, Late Mississippian prodeltaic rhythmites in the Appalachian Basin: a hierarchical record of tidal and climatic periodicities: Journal of Sedimentary Research, v. 67, p. 653–660.

O'BRIEN, D.J., WHITEHOUSE, R.J.S., AND CRAMP, A., 2000, The cyclic development of a macrotidal mudflat on varying timescales: Continental Shelf Research, v. 20, p. 1593–1619.

PRAVE, A.R., DUKE, W.L., AND SLATTERY, W.S., 1996, A depositional model for storm- and tide-influenced prograding siliciclastic shorelines from the Middle Devonian of the central Appalachian foreland basin, U.S.A.: Sedimentology, v. 43, p. 611–629.

REINECK, H.E., AND GERDES, G., 1997, Tempestites in Recent shelf and tidal environments of the southern North Sea: Courier Forschungsinstitut Senckenberg, v. 201, p. 361–370.

REINECK, H.E., AND SINGH, I.B., 1980, Depositional Sedimentary Environments, Second Edition: Berlin, Springer-Verlag, 549 p.

SHI, Z., 1991, Tidal bedding and tidal cyclicities within the intertidal sediments of a microtidal estuary, Dyfi River Estuary, west Wales, U.K.: Sedimentary Geology, v. 73, p. 43–58.

SONETT, C.P., FINNEY, S.A., AND WILLIAMS, C.R., 1988, The lunar orbit in the later Precambrian and the Elatina sandstone laminae: Nature, v. 335, p. 806–808.

TESSIER, B., 1993, Upper intertidal rhythmites in the Mont-Saint-Michel Bay (NW France): Perspectives for paleo-reconstruction: Marine Geology, v. 110, p. 355–367.

TESSIER, B., AND GIGOT, P.A., 1989, Vertical record of different tidal cyclicities: an example from the Miocene Marine Molasse of Digne: Sedimentology, v. 36, p. 767–776.

VAN DEN BERG, J.H., 1981, Rhythmic seasonal layering in a mesotidal channel fill sequence, Oosterschelde Mouth, The Netherlands, *in* Nio, D.-D., Shuttenhelm, R.T.E., and van Weering, Tj.C.E., eds., Holocene Marine Sedimentation in the North Sea Basin: International Association of Sedimentologists, Special Publication 5, p. 147–159.

VISSER, M.J., 1980, Neap–spring cycles reflected in Holocene subtidal large-scale bedform deposits a preliminary note: Geology, v. 8, p. 543–546.

WELLS, J.T., ADAMS, C.E., JR., PARK, Y.A., AND FRANKENBERG, E.W., 1990, Morphology, sedimentology and tidal channel processes on a high-tide-range mudflat, west coast of South Korea: Marine Geology, v. 95, p. 111–130.

WILLIAMS, G.E., 1998, Precambrian tidal and glacial clastic deposits: implications for Precambrian Earth–Moon dynamics and paleoclimate: Sedimentary Geology, v. 120, p. 55–74.

YANG, C., AND NIO, S., 1985, The estimation of palaeohydrodynamic processes from subtidal deposits using time-series analysis methods: Sedimentology, v. 32, p. 41–57.

YU, G.H., 1996, Stratigraphy (lithostratic) of Zhejiang Province: Wuhan, China University of Geosciences Press, 236 p. (in Chinese).

ZHOU, M.K., WANG, R.Z., AND LI, Z.M., 1993, Ordovician to Silurian lithofacies, paleogeography and mineralization in South China: Beijing, Geological Publishing House, 111 p. (in Chinese with English abstract).

Received 3 January 2003; accepted 3 January 2004.